70-GT-106

Printed in U.S.A.

an ASME publication

$2.00 PER COPY

$1.00 TO ASME MEMBERS

Experimental Performance in Annular Cascade of Variable Trailing-Edge Flap, Axial-Flow Compressor Inlet Guide Vanes

T. H. OKIISHI

Assistant Professor,
Assoc. Mem. ASME

G. H. JUNKHAN

Associate Professor,
Assoc. Mem. ASME

G. K. SEROVY

Professor and Assistant Director,
Assoc. Mem. ASME

Mechanical Engineering and
Engineering Research Institute,
Iowa State University,
Ames Iowa

Aerodynamic performance of a variable-geometry axial-flow compressor inlet guide vane configuration for a gas turbine unit was determined in a series of annular cascade tests. The variable-geometry vanes used uncambered, symmetrical airfoil sections as the basic blade profile with the rear 70 percent of the vane profile movable as a trailing-edge flap. Vane flap mechanical setting angles of 0 to 50 deg measured from the axial direction were possible, and performance parameters were determined over this range of angles. Turning angles followed a general trend obtained with Carter's rule for accelerating cascades with the presently measured values tending to be lower than those obtained with Carter's rule at higher setting angles. For large camber angles (greater than 35 deg) zero-incidence blade element total-pressure loss coefficients for the 50 percent passage location of the flapped vanes tested were higher than those that might have been obtained with a continously cambered vane row of the same solidity and camber.

Contributed by the Gas Turbine Division of The American Society of Mechanical Engineers for presentation at the ASME Gas Turbine Conference & Products Show, Brussels, Belgium, May 24-28, 1970. Manuscript received at ASME Headquarters, January 30, 1970.

Copies will be available until March 1, 1971.

Experimental Performance in Annular Cascade of Variable Trailing-Edge Flap, Axial-Flow Compressor Inlet Guide Vanes

T. H. OKIISHI G. H. JUNKHAN G. K. SEROVY

INTRODUCTION

Control of the performance characteristics of axial-flow compressor units by variable geometry is not a new concept. During the past 20 years, a number of aircraft, industrial, and research compressors have incorporated some means for varying the stagger angle and/or the effective camber of one or more blade rows. Serovy and Kavanagh (1)[1] have reviewed the literature in this area and have commented on the present status of variable geometry applications.

The principal goal of using variable geometry has been to modify the overall performance of a compressor under off-design operating conditions. In gas turbine units, it has been necessary to restructure the compressor performance at reduced rotational speeds so the equilibrium engine operating line does not pass through regions of unstable compressor operation. Although not emphasized, a secondary reason for use of variable geometry is the optimization of compressor performance for off-design engine operation.

Probably the simplest form of variable geometry and the easiest to design and evaluate is that involving control by adjustable inlet guide vanes. Multistage axial-flow compressors for a number of commercial and military aircraft gas turbines have employed this system (1). However, all documented applications have used initially cambered guide vanes for design-point velocity diagrams and have simply provided for resetting the vanes by mechanically rotating them about the blade mounting axis to increase the angle of incidence. This form of resetting changes the vane incidence by a uniform amount along the vane span and ordinarily does not result in a favorable pattern of incidence change on a downstream rotor row. As pointed out by Steinke and Crouse (2), a vane form, which would give a reasonable spanwise variation of rotor velocity diagrams under off-design operating conditions, would probably be more complicated. The National Aeronautics and Space Administration sponsored fabrication and evaluation of two possible variable camber guide vane configurations (3). As shown in Fig.1, while both configurations were designed to form identical continuously cambered vanes in the fully cambered position, their geometries differed otherwise. The mean radius loss coefficient and turning angle were reported to be 0.017 and 26.7 deg, respectively, for both vanes for inlet Mach number of 0.22 during fully cambered operation. Mean-radius loss coefficients of 0.021 and 0.069 were reported for axial flow operation (inlet Mach number of 0.30) for vanes A and B of Fig.1, respectively.

---

[1] Numbers in parentheses designate References at end of paper.

NOMENCLATURE

- a = position of maximum camber along chord line from leading edge
- c = chord length
- r = radius, ft
- U = blade velocity, fps
- V = fluid velocity, fps
- β = air angle measured from axial direction, deg
- γ = vane flap setting angle, deg
- δ = deviation angle, deg
- σ = blade-row solidity, chord length/circumferential spacing at row outlet
- ϕ = camber angle
- $\bar{\omega}$ = blade-element total-pressure loss coefficient

Subscripts

- t = tip
- z = axial component
- 1 = guide vane inlet station
- 2 = guide vane exit or rotor inlet station

Superscript

- $'$ = relative to coordinates rotating with rotor at rotor inlet

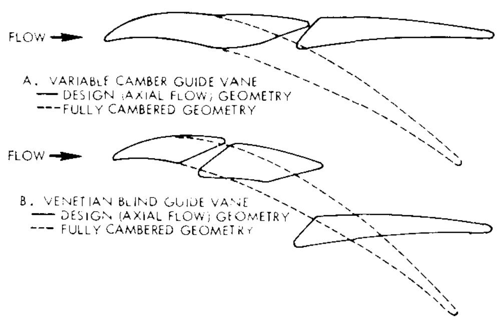

Fig.1 Guide vane configurations of reference (3)

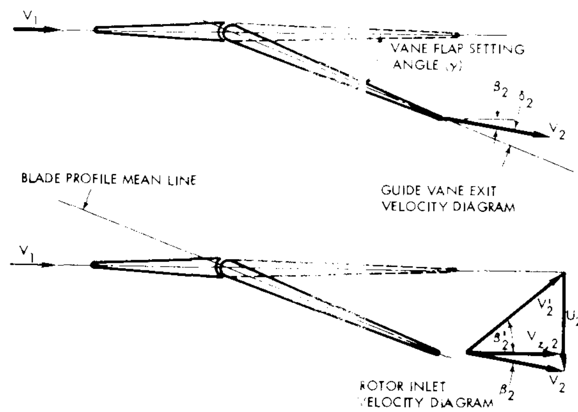

Fig.2 Sketch of variable trailing-edge flap, inlet guide vane profile

For simplicity, an initially uncambered airfoil section was used as the basic guide vane blade element profile for the presently tested set of inlet guide vanes with the rear portion of each vane acting as a trailing-edge flap. The differences between these vanes and those of reference (3) are seen by comparing Figs.1 and 2. Although the vane incidence would remain zero, the effective camber of the vane section and the stagger angle could be changed, and the prerotation of the air, thus produced at the rotor entrance, was expected to modify compressor performance so satisfactory off-design engine operation could be achieved. As tested, the vanes could be set for a maximum vane flap setting angle of 53 deg from the compressor axis in the direction of compressor rotation. The primary purpose of the tests was to evaluate, in terms of turning and losses, the performance of the flapped guide vanes. The tests were conducted in the Turbomachinery Components Research Laboratory of the Engineering Research Institute, Iowa State University during the period September 1967 to March 1968.

This paper describes the experimental facility developed for the test program and results which may be important to compressor designers in future applications of similar vane geometries.

GUIDE VANE DESCRIPTION

At the compressor design operating point, the guide vanes were scheduled to operate as uncambered symmetrical airfoils at zero incidence. The vane profile under this condition was based on NACA 0010 airfoil coordinates with each thickness coordinate reduced by 50 percent, producing a maximum thickness-chord ratio of 5 percent. Thirteen vanes were specified, and chord length was varied along the span to give an approximately constant solidity of 1.07 to 1.08. The flapped section involved the rear 70 percent of the blade section. A sketch of the vane section is shown in Fig.2. Other pertinent characteristics of the guide vanes are included in the following section.

EXPERIMENTAL INVESTIGATION

Apparatus

The general apparatus is shown in Fig.3. Atmospheric air entered a large sealed settling chamber and passed through a 5-ft-square inlet tank in which several turbulence-damping screens were located. The screens, proceeding in a downstream direction, were a 0.375-in. mesh hardware cloth followed 25 in. downstream by a copper wire screen with a 0.033-in. mesh and 0.0075-in. wire diameter. A second copper screen of the same mesh and wire diameter was located 12.5 in. further downstream. The last screen was positioned 11.5 in. upstream of the upstream face of a fiberglass contraction section inlet to the annular cascade.

The annular cascade consisted of 13 guide vanes equally spaced circumferentially with hub-tip ratios of 0.496 at the leading edge and 0.648 at the trailing edge (hub end) of the vanes when the vanes were set for no turning (vane flap setting angle, 0 deg). Vane positions, relative to center body support struts, are shown in Fig.4. Wake data were obtained from surveys behind No. 1 guide vane, whose position is indicated in Fig.4. A constant tip casing radius was maintained throughout the length of the cascade and downstream test fixture. The hub diameter increased through the length of the cascade and part way into the downstream test fixture. The movable flap surface was turnable through a maximum angle of 53 deg with the axial centerline of the annular configuration. Angular positions of the guide vane flaps were set on a guillotine-type fixture with the entire blade row removed from the cascade. Each blade was individually rotated to position and positively locked mechanically by a device on the vane turning axis. Conformity of the flap to the guillotine reference was checked by placing a strong light so that the operator could detect any

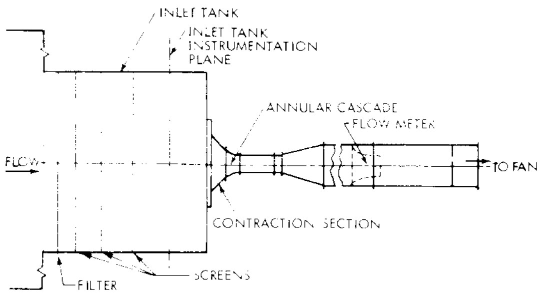

Fig.3 Sketch of the test apparatus

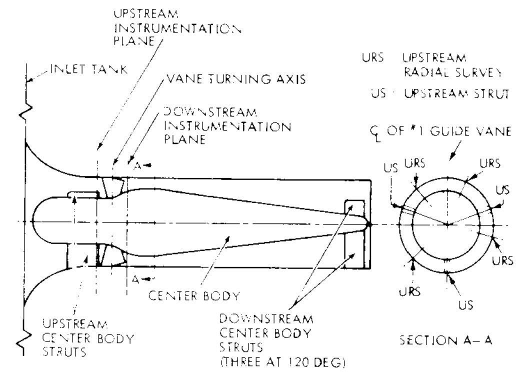

Fig.4 Annular cascade system

mismatch between the guillotine and the flap surfaces.

Downstream from the annular casing the air proceeded through a 7-deg conical annular diffuser with a casing diameter equaling that of the test cascade, then through a nonannular diffuser followed by a flow metering section consisting of a stacked-tube straightener and a 7-in. throat-diameter flow nozzle. From the nozzle, air flowed into a stilling chamber at the inlet to a 13,000 cfm, 20.0-in. head rise fan. Flow rates were controlled by fan inlet guide vanes.

Instrumentation

Four probe holes for radial surveys of total pressures of the inlet flow to the blade row and four static pressure taps were located in the outer casing upstream of the guide vanes in the upstream instrumentation plane as shown in Fig.4. The upstream instrumentation plane was located approximately 72 percent of the mid-passage chord upstream of the vane turning axis. Two probe holes and four static pressure taps were located in the rotatable, specially fitted outer casing in the downstream instrumentation plane, while four circumferentially spaced and stationary static pressure taps were installed in the hub in the same plane. The downstream instrumentation plane was located approximately 85 percent of the mid-passage chord downstream of the vane turning axis.

Because the test cascade was on the suction side of the fan, all pressures were read from manometers in inches of water below atmospheric pressure. Manometer scales were checked against a micromanometer standard.

Upstream surveys were made with Kiel probes, while downstream radial surveys of total pressure and flow angle were made with United Sensor and Controls Corporation model CA "cobra" probes.

Radial survey positions, set with motorized probe positioners, were read from the positioner control panel with frequent checks on the positioner counters themselves. Initial calibration of the control panel indicator and the counters was performed with micrometer gages inserted between the probe and the test fixture.

Probe flow angle orientations for blade wake surveys were read from the positioner counters only. Balance of the outside hole pressures on the cobra survey probes was checked with a U-tube water manometer for all measurements reported. The survey probe instrumentation system was estimated to measure probe angular position to ± 1 deg. Circumferential angular positions of the downstream radial survey probes were read from a scale and fiduciary marks engraved on the outside of the test section. The least count of the scale was 0.5 deg.

Since flow angles in the vaneless passage were found to be virtually constant and axial except in the boundary layers and upstream support strut wakes, the zero angle reference datum for each probe was determined during vaneless passage tests.

Inlet tank temperatures were obtained from millivolt potentiometer readings of the electrical potential of a copper-constantan thermocouple.

Test Procedure

Upstream total pressures were measured at 10, 30, 50, 70, and 90 percent of the passage height from the outer casing wall. Downstream total pressures and flow angles were measured at 10, 30, 50, 70, and 90 percent of the passage height from the outer casing wall and enough circumferential locations at each radial location to define one complete vane wake.

Average exit total pressures for each radial position were determined by mechanical integration of the wake total pressure profiles. Average free-stream flow angles were interpreted as being representative guide vane outlet air angles.

The inlet Mach number range for the tests was 0.13 to 0.38. Data were obtained for unchoked flow only in all cases.

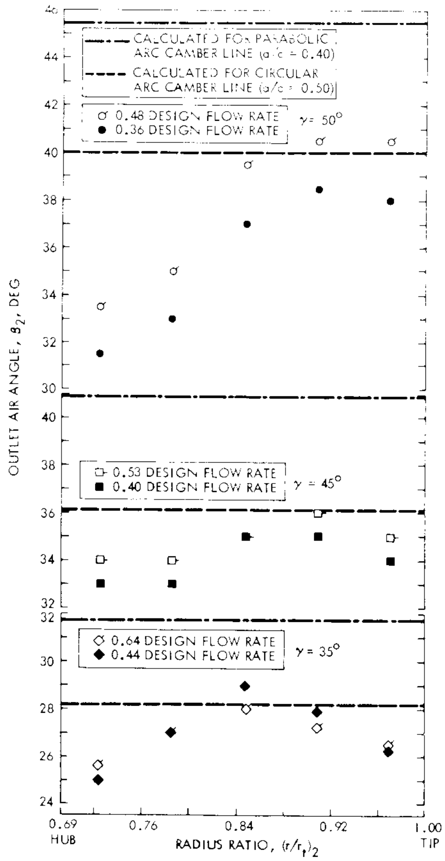

Fig.5(a) Radial variation of outlet air angle for γ = 50, 45, and 35 deg

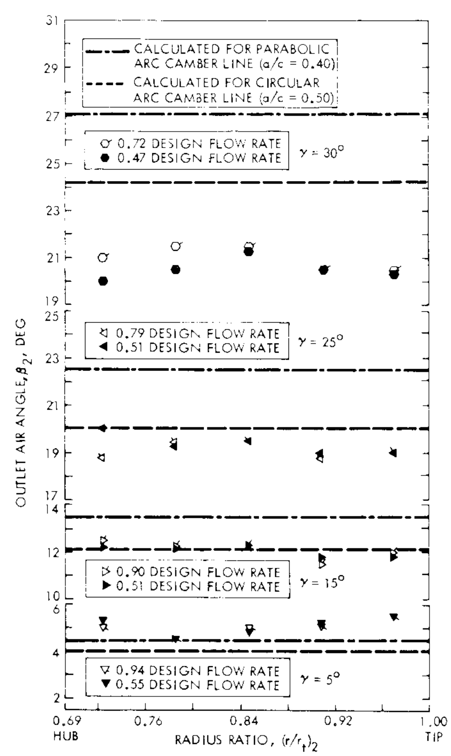

Fig.5(b) Radial variation of outlet air angle for γ = 30, 25, 15, and 5 deg

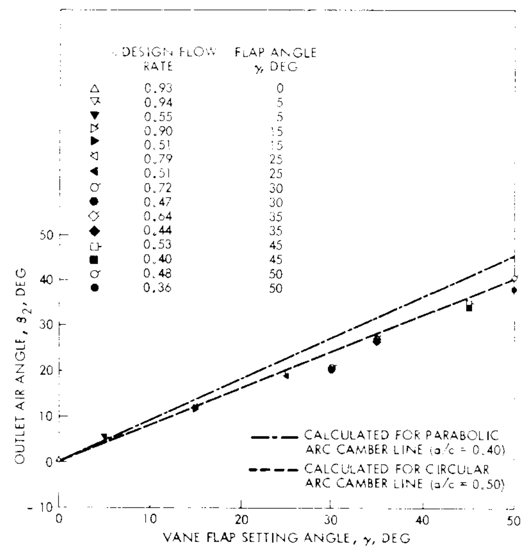

Fig.6 Measured values of outlet angle as a function of vane flap setting angle for measuring station located at 10 percent of the passage height from the outer casing ($(r/r_t)_2$ = 0.9694) compared with Carter's rule values

RESULTS

Outlet Angle

Fig.5 shows the radial variation of measured blade element outlet air angle for different flap angles. For comparison, outlet air angles for optimum incidence (maximum lift/drag ratio) obtained with Carter's rule (4) for accelerating cascades are shown. One set of Carter's rule values was obtained for circular-arc mean camber line (maximum camber at 50 percent of chord length) blades, while the other was determined for parabolic-arc mean camber line (maximum camber at 40 percent of chord length from leading edge) blades. The variation of the measured outlet angle with radius appeared to be reasonably uniform for vane flap setting angles less than 25 deg. At larger flap angles, the measured outlet angles associated with the hub region tended to be smaller than those measured in the mid-passage and tip regions. This effect can be explained mainly in terms of secondary flows and appears to be consistent with the results of Lieblein and Ackley (5). More suppression of turning in the hub region than in the tip region at the larger flap angles, due to the larger vane end-wall clearance formed in the hub region, also aupports the trend shown.

Figs.6 to 8 show the variation of blade element outlet angle with vane setting angle for the blade elements associated with the 10, 50, and 90

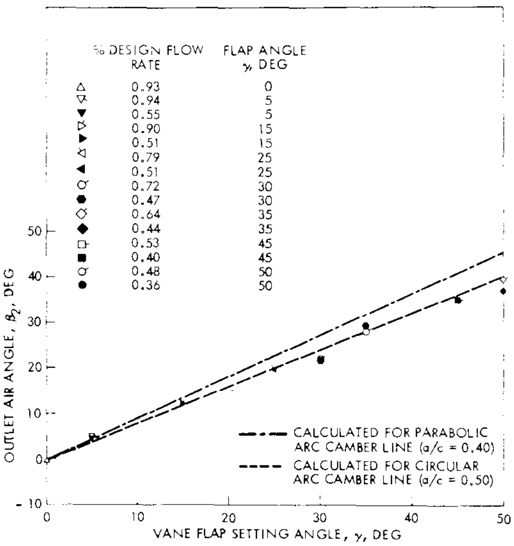

Fig.7 Measured values of outlet angle as a function of vane flap setting angle for measuring station located at 50 percent of the passage height from the outer casing ($(r/r_t)_2 = 0.8468$) compared with Carter's rule values

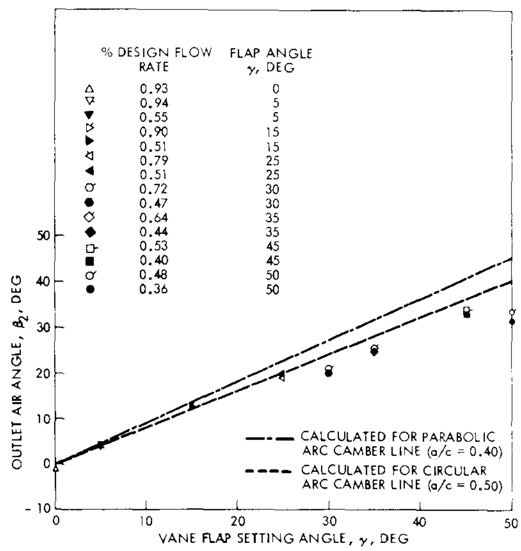

Fig.8 Measured values of outlet angle as a function of vane flap setting angle for measured station located at 90 percent of the passage height from the outer casing ($(r/r_t)_2 = 0.7243$) compared with Carter's rule values

percent passage height from the outer casing locations at each experimental flow rate. These figures also compare the experimental outlet angle data obtained with values obtained with Carter's rule (4). Experimental outlet angle data generally followed the trend obtained with Carter's rule, with measured values close to the Carter's rule values obtained for a circular-arc camber line blade section.

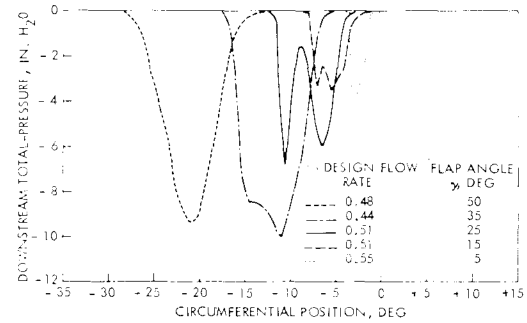

Fig.9 Blade element wake total pressure survey data for $(r/r_t)_2 = 0.9694$ (10 percent of the passage height from the outer casing)

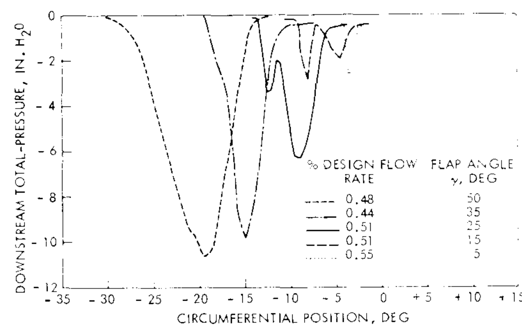

Fig.10 Blade element wake total pressure survey data for $(r/r_t)_2 = 0.7243$ (90 percent of the passage height from the outer casing)

Total Pressure

As shown in Figs.9 and 10, during the tests associated with the vane setting angles from 15 to 35 deg, double total-pressure wakes were detected in the hub and tip regions downstream from a single vane. It is likely that the effect was mainly caused by leakage of fluid through the vane end clearances from the pressure surface to the suction surface. The absence of double wakes at flap angles greater than 35 deg is explainable in terms of the leaking fluid having adequate distance (distance between vane trailing edge and measuring plane increased with increase in flap angle) to distribute itself enough so that it was no longer distinct. The figures also illustrate the general tendency toward larger wakes as flap angle is increased.

Average Loss Coefficient

Fig.11 shows the hub-to-tip variation of the total pressure loss coefficient for three vane setting angles. Except for vane setting angles 1 less than 15 deg, losses were appreciably larger near the hub and tip regions than elsewhere in the passage. Fig.12 shows variation of the average total pressure loss coefficient with vane setting angle for the blade elements associated with the

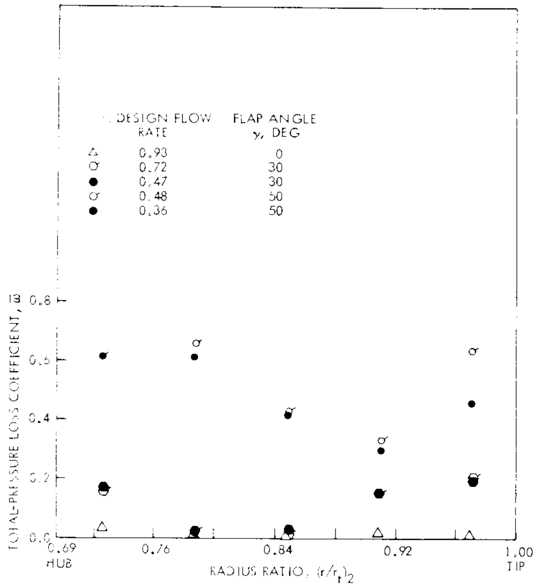

Fig.11 Radial variation of total-pressure loss coefficient for γ = 0, 30, and 50 deg

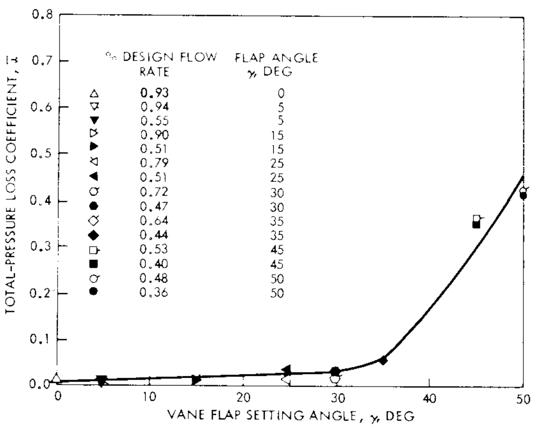

Fig.12 Measured values of total-pressure loss coefficient as a function of vane flap setting angle for measuring station located at 50 percent of the passage height from the outer casing $((r/r_t)_2=0.8468$

50 percent passage height from the outer casing location at each experimental flow rate. The solid line shows an attempt to graphically smooth the data. A marked increase in loss is observed for flap angles greater than approximately 35 deg. In general, the loss data showed little dependence on inlet Mach number over the test range covered.

Fig.13 compares the present average loss-coefficient data for the mid-passage location and some low-speed two-dimensional cascade loss-coefficient data for σ = 1.0 collected by other investigators. Note that camber angle for the flapped vanes is identical to flap angle. Ackeret's (6) data are for uncambered blades and zero turning. Dunavant's (7) data are for two sets of cambered

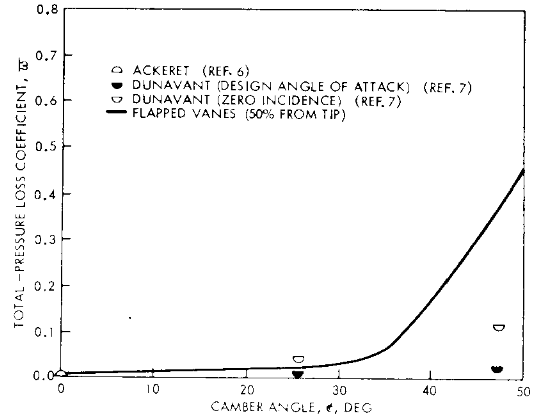

Fig.13 Comparison of flapped guide vane total-pressure loss coefficient data with those for conventionally cambered guide vane airfoil sections having equivalent values of row solidity

blades. In the case of Dunavant's data, two data points are shown for each of his configurations. One is the design-angle-of-attack value, while the other is an estimate of the zero-incidence-angle value. Camber angles and the zero incidence condition for Dunavant's vanes were obtained by considering mean camber line shape at the 0.5 and 95 percent chord locations. It seems clear from the comparison that for large camber angles (ϕ > 35 deg) smoothly cambered vanes are superior losswise to the flapped vanes investigated.

CONCLUSIONS

For the particular trailing-edge flap vane geometry studied, the principal conclusions are:

1 The turning angle data generally followed trends obtained with Carter's rule for accelerating cascades with the experimental values tending to be lower than those obtained with Carter's rule at the higher setting angles. The rule values for a circular-arc mean camber line blade section more nearly approximated the experimental data than the rule values for a parabolic-arc mean camber line blade section. For the largest vane setting angle (γ = 50 deg) approximately 38 deg of turning was possible.

2 For the mid-passage blade element, average loss coefficients were small for flap angles less than approximately 35 deg (about 28 deg of turning). A marked increase of loss coefficient was observed for larger flap setting angles.

The data results may be used to improve design control and input information in axial flow compressor design. The outlet angles and loss coefficients measured for the guide vanes in the cambered positions are essential in fixing the amount of guide vane reset needed to change compressor off-design performance (and to determine whether the desired change is possible). In addition, the measured guide vane characteristics would be of material importance in any program for estimating overall and blade-row performance of a compressor unit utilizing such guide vanes. It is emphasized that the flapped guide vanes tested were a trial set, and no claim is made for their representing an optimum design.

REFERENCES

1 Serovy, G. K. and Kavanagh, P., "Considerations in the Design of Variable-Geometry Blading for Axial-Flow Compressor Stages," NATO Advisory Group for Aerospace Research and Development, AGARD CP No. 34 (1968).

2 Steinke, R. J. and Crouse, J. E., "Preliminary Analysis of the Effectiveness of Variable-Geometry Guide Vanes to Control Rotor-Inlet Flow Conditions," US NASA TN D-3823 (1967).

3 Linder, C. G. and Jones, B. A., "Single-Stage Experimental Evaluation of Variable Geometry Guide Vanes and Stators. Part II — Annular Cascade Investigations of Candidate Variable Geometry Designs," US NASA CR-54555 (1967).

4 Carter, A. D. S., "The Low-Speed Performance of Related Airfoils in Cascades," Great Britain ARC C. P. No. 29 (1950).

5 Lieblein, S. and Ackley, R. H., "Secondary Flows in Annular Cascades and Effects on Flow in Inlet Guide Vanes," US NACA RM E51G27 (1951).

6 Ackeret, J., "Aspects of Internal Flow," In Sovran, G., ed. Fluid Mechanics of Internal Flow, Elsevier Publishing Co., New York (1967).

7 Dunavant, J. C., "Cascade Investigation of a Related Series of 6-Percent-Thick Guide-Vane Profiles and Design Charts," US NACA RML54I02 (1954).